Contrib Mineral Petrol (2003) 146: 341–355
DOI 10.1007/s00410-003-0502-x

ORIGINAL PAPER

Daniela Rubatto · Marco Scambelluri

U-Pb dating of magmatic zircon and metamorphic baddeleyite in the Ligurian eclogites (Voltri Massif, Western Alps)

Received: 30 January 2003 / Accepted: 2 July 2003 / Published online: 8 August 2003

Abstract U-Pb geochronology with ion microprobe (SHRIMP) analysis has been carried out on eclogite-facies rocks of the Beigua Unit, an ophiolitic slice of the Voltri Massif, Western Alps. The investigated samples are eclogites and high-pressure metasomatic rocks (metarodingites and centimetre-sized Ti-clinohumite-bearing dykes). Zircon contained in an eclogitic metagabbro and a metarodingite preserves magmatic zoning patterns and trace element compositions. The zircon ages of 160 ± 1 and 161 ± 3 Ma are interpreted to date the crystallization of the gabbroic protoliths. Ti-clinohumite dykes in the same unit contain baddeleyite crystals in textural equilibrium with Ti-clinohumite, diopside, chlorite and magnetite, which form the eclogite-facies assemblage in these rocks. Baddeleyite also contains inclusions of such minerals, indicating its formation at high pressure. The baddeleyite has cathodoluminescence intensity and chaotic patterns similar to metamorphic zircon. It contains a significant amount of Hf (1.3–1.7 wt%), traces of Ti, Y, Nb, Ta, REE, U and Th. Its chondrite-normalised trace element pattern has strong enrichment in middle REE, positive Ce-anomaly and small negative Eu-anomaly. This represents the first report of baddeleyite formed during regional metamorphism, and suggests that this mineral could (re)crystallize easier than zircon under low-temperature, high-pressure conditions. The age of the baddeleyite is interpreted as likely dating the eclogite-facies metamorphism in the Beigua Unit at 33.6 ± 1.0 Ma. This age is very close to the Early Oligocene age of the overlying Tertiary continental breccias and conglomerates, which contains clasts of high-pressure rocks. This sedimentary record, which is unique for Alpine high-pressure units, is direct evidence of fast exhumation of the Beigua eclogites. The young age for the HP metamorphism of the Beigua ophiolite makes a revision of either the palaeogeography prior to collision, or of the subduction setting in the entire region, necessary.

Editorial responsibility: J. Hoefs

D. Rubatto (✉)
Research School of Earth Sciences and Department of Geology, Australian National University, 0200 Canberra, Australia
E-mail: daniela.rubatto@anu.edu.au

M. Scambelluri
Dipartimento per lo Studio del Territorio e delle sue Risorse, Università di Genova, Corso Europa 26, 16132 Genova, Italy

Introduction

The ophiolite units and the eclogite-facies rocks of the Alps have long been the subject of intense geochronological study. In recent years, the application of new isotopic techniques has allowed precise dating of mineral that formed during high-pressure (HP) events. It has become possible to date HP metamorphism in mafic rocks and in low-temperature eclogites, which is a notoriously difficult task (Inger et al. 1996; Dûchene et al. 1997; Gebauer et al. 1997; Liati and Gebauer 1999; Rubatto et al. 1999; Rubatto and Hermann 2001; Agard et al. 2002; Rubatto and Hermann 2003). An increasing number of geochronological data on Alpine eclogites suggests a trend in age distribution, with subduction getting younger from the internal to the external part of the chain (Inger et al. 1996; Dûchene et al. 1997; Gebauer et al. 1997; Rubatto et al. 1998; Liati et al. 2003), i.e. from tectonic slices derived from the African margin to the ones derived from the European margin. The oldest eclogites pertain to the Austroalpine Units of the Western Alps (65–69 Ma, Inger et al. 1996; Dûchene et al. 1997; Rubatto et al. 1999); the age of eclogite-facies metamorphism in the ophiolites is at ~45 Ma (Rubatto et al. 1998; Rubatto and Hermann 2003), whereas high- to ultrahigh-pressure metamorphism in the external portions of the western Alpine belt is very young in age, i.e. Oligocene (Dûchene et al. 1997; Gebauer et al. 1997; Rubatto and Hermann 2001). The deep formation and the subsequent surface exposure of the latter rock units requires very fast exhumation rates as high as

2–4 cm/year (Dûchene et al. 1997; Gebauer et al. 1997; Rubatto and Hermann 2001). These recently proposed models and data are a matter of vigorous debate (cf. Dûchene et al. 1997; Gebauer et al. 1997; Rubatto et al. 1998; Rubatto and Hermann 2001 versus Agard et al. 2002), and more work is needed to test their validity.

Within this framework, the geochronological study of the eclogitic metaophiolites of the Voltri Massif, in the Ligurian Western Alps, adds important constraints to the petrological and tectonic models of eclogite formation and exhumation in the Alpine belt. Because of its location, the presence of metaophiolite that preserve eclogite-facies assemblages, and because it is directly overlain by Tertiary sediments, the Voltri Massif represents an ideal setting to test the current model on Tethys formation and Alpine subduction youngening toward the external units.

The technique used (U-Pb dating of mineral zones) ensures dating of single events and avoids the problem of local disequilibrium, a common feature in low temperature rocks. Metamorphic baddeleyite, a mineral never found before in eclogites, is dated here for the first time in HP rocks. The geochronological data are combined with chemical data and textural analysis, as well as with the available petrologic knowledge of the rock unit, to relate age with metamorphic conditions. The comparison between the timing of sedimentation and the age of the eclogites places constraints on the exhumation and erosion rates of Alpine HP rocks and on the tectonic evolution of the Western Alps.

Geological background

The Voltri Massif is a nappe of ophiolite and associated metasediments that underwent the Alpine subduction and exhumation cycle. It is located in the southeastern end of the Alpine arc, at the boundary with the Apennine (Fig. 1). To the east, the Voltri ophiolites are separated from the Apennines by the Sestri Voltaggio Zone, a composite terrain consisting of Triassic-Liassic carbonate rocks and of dismembered Mesozoic ophiolites showing peak Alpine blueschist assemblages (Cortesogno and Haccard 1984). To the west, the Voltri Massif overlies the Hercynian gneisses, amphibolites and granitoids of the continental European Savona crystalline basement, which locally underwent greenschist- to blueschist-facies Alpine metamorphism (Messiga 1987). Towards the north and northeast, the Voltri Massif is bounded by the Tertiary sediments of the Piemonte Basin, whose basal breccias and conglomerates include clasts of HP metaophiolites (Cortesogno and Haccard 1984). The lowermost parts of these sedimentary sequences underwent short-range transport and have been dated at the Priabonian to Rupelian (about 35 to 30 Ma, chronological scale of Harland et al. 1989) on the base of paleontological and stratigraphical records (Charrier et al. 1964; Lorenz 1979; Gelati et al. 1993, 1998; Di Biase et al. 2002).

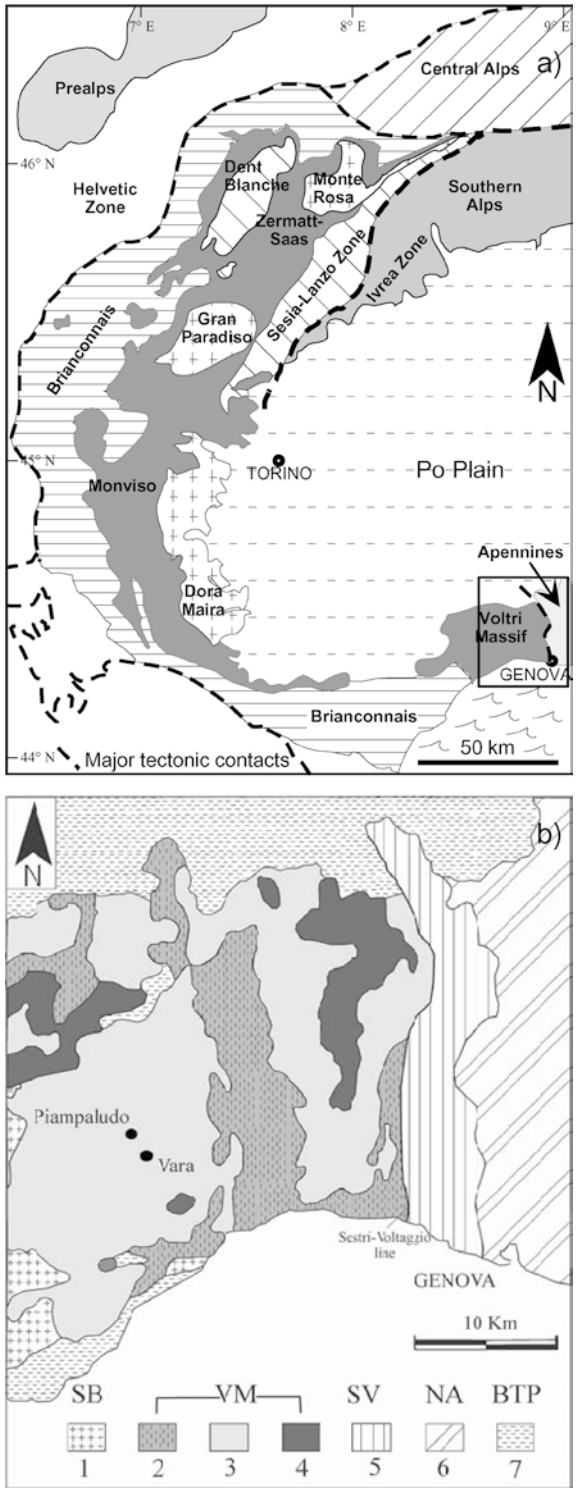

Fig. 1 a Geological sketch map of the Western Alps. The ophiolitic units are in *dark grey*. The *square* indicates the Voltri Massif, represented in **b**. **b** Geological sketch map of the Voltri Massif. *SB* Savona crystalline basement; *VM* Voltri Massif; *1* metasedimentary units; *2* Beigua serpentinite unit; *3* Erro Tobbio peridotite; *SV* Sestri Voltaggio Zone; *NA* Northern Apennine units; *BTP* Tertiary sediments of the Piemontese Basin

Slices from different lithospheric levels (lithospheric subcontinental mantle, oceanic lithosphere and sediments, continental margins) were tectonically coupled together in the Voltri Massif during the Alpine orogeny (Chiesa et al. 1975; Vissers et al. 1991). The Voltri tectonic units are subdivided as follows (Fig. 1b): (1) Beigua Unit, consisting of antigorite serpentinites and eclogitic metagabbros, from precursor oceanic peridotites and MORB-type gabbros (dominant Fe-Ti-rich gabbros); (2) Voltri-Rossiglione, Ortiglieto and Alpicella Units, consisting of calcschists and metavolcanics derived from oceanic sediments and MORB-type lava flows; (3) Erro-Tobbio peridotites, consisting of HP serpentinites and metaperidotites, which preserve km-scale volumes of their pre-Alpine mantle peridotite protoliths, and subordinated MORB metagabbros and metabasalts.

Despite the large number of detailed field and petrological work done in the Voltri Massif (Ernst 1976; Messiga and Scambelluri 1991; Liou et al. 1998; Scambelluri and Rampone 1999; Capponi and Crispini 2002), these HP ophiolites have not been dated so far. This lack of geochronological data for the Voltri, particularly U-Pb data, is partly due to the fact that eclogitisation occurred at particularly low temperature (400–500 °C) when compared with other eclogite-facies units in the Alps. In fact, it was long believed that at this temperature (re)crystallization of U-Pb minerals did not occur.

Sample description

The rocks studied here are eclogites and HP Ca- and Mg-enriched metasomatic rocks (rodingites and Ti-clinohumite-bearing dykes). Zircon-bearing samples were selected from a larger number of rock types, including also Mg-gabbros. Samples were collected at the localities of Vara and Piampaludo within the Beigua Unit (Fig. 1b) which mostly consists of serpentinites enclosing metre-sized bodies of eclogites, minor bodies of metarodingite and thin brownish centimetre-sized dykes rich in Ti-clinohumite. The serpentinites have an antigorite + olivine + Ti clinohumite mineral assemblage that has been shown to develop at eclogite-facies conditions and that represents the highest (peak) metamorphic grade found in the area (Cimmino et al. 1981). The investigated eclogites and metasomatized rodingites and Ti-clinohumite-bearing dykes have been the subject of a number of petrologic and geochemical studies. Detailed information on the microtexture and composition of bulk rocks and minerals is given by Cimmino et al. (1981), Messiga and Scambelluri (1991), Messiga et al. (1995), Liou et al. (1998), and Scambelluri and Rampone (1999).

BVM eclogitic metagabbro

Eclogite BVM is part of a large (a 100-m-long and several metres thick) body with mylonitic to tectonitic structures that crops out in the area of Vara (Fig. 1b). This rock displays a compositional layering determined by alternating omphacite rich-layers with layers dominated by garnet porphyroblasts. Thin rutile bands parallel the eclogitic foliation are present in these eclogites. The omphacite-rich layers consist of omphacite porphyroclasts in a finer-grained matrix composed of neoblastic omphacite associated with garnet crystals (Fig. 2A). The sodic pyroxene porphyroclasts (aegirine-augite) contain thin rutile micro-inclusions and represent an early (prograde) generation of eclogitic clinopyroxene (omphacite I). These omphacite porphyroclasts are dissected along the mylonitic foliation and are extensively replaced by fine-grained omphacite II, which is richer in jadeite end-member (Messiga and Scambelluri 1991). Like the clinopyroxene, two different generations of garnet are present in the rock (porphyroblasts and finer-grained idioblastic garnets), indicating that the eclogitic event comprises two main episodes of recrystallization, the first being likely prograde (Messiga and Scambelluri 1991). Small patches of secondary glaucophane locally replace omphacite and appear in equilibrium with garnet neoblasts enriched in grossular component (Messiga and Scambelluri 1991).

The occurrence of millimetre-sized, sodic clinopyroxene porphyroclasts (locally preserving relic cores of igneous Ti-augite), as well as the mineralogical and chemical compositions of these eclogites points to Fe-Ti-rich gabbroic precursor (Mottana and Bocchio 1975). The rock underwent peak metamorphism at 13 kbar and 450–500 °C (Ernst 1976; Messiga and Scambelluri 1991). Higher pressure-temperature estimates (18 kbar, 550 °C) have been recently proposed by Liou et al. (1998) based on the coexistence of omphacite and talc.

MF high-pressure metarodingite

The selected metarodingite is part of a metre-thick dyke in the area of Vara (Fig. 1b). This rock displays a diopside + chlorite + grossular-rich garnet assemblage (Fig. 2B) with subordinated magnetite, titanite and apatite. Garnet is concentrated in the centre of the dike, whereas chlorite is abundant at the rim. The rock contains large relict clinopyroxene domains (Ti-augite) surrounded by fine-grained domains of chlorite, garnet and diopside (Fig. 2B). These domains are interpreted to correspond to coarse igneous clinopyroxene and plagioclase domains of the original gabbroic rock. In some places, the titanite crystals include relict igneous ilmenite. The widespread preservation of igneous Ti-augite, apatite, Fe-oxides as well as of coarse igneous textures indicates a differentiated Fe-Ti-rich gabbroic protolith.

M1 and AF Ti-clinohumite metagabbroic dykes

The selected samples are the cores of several tens of centimetre-thick dykes within the serpentinite of the

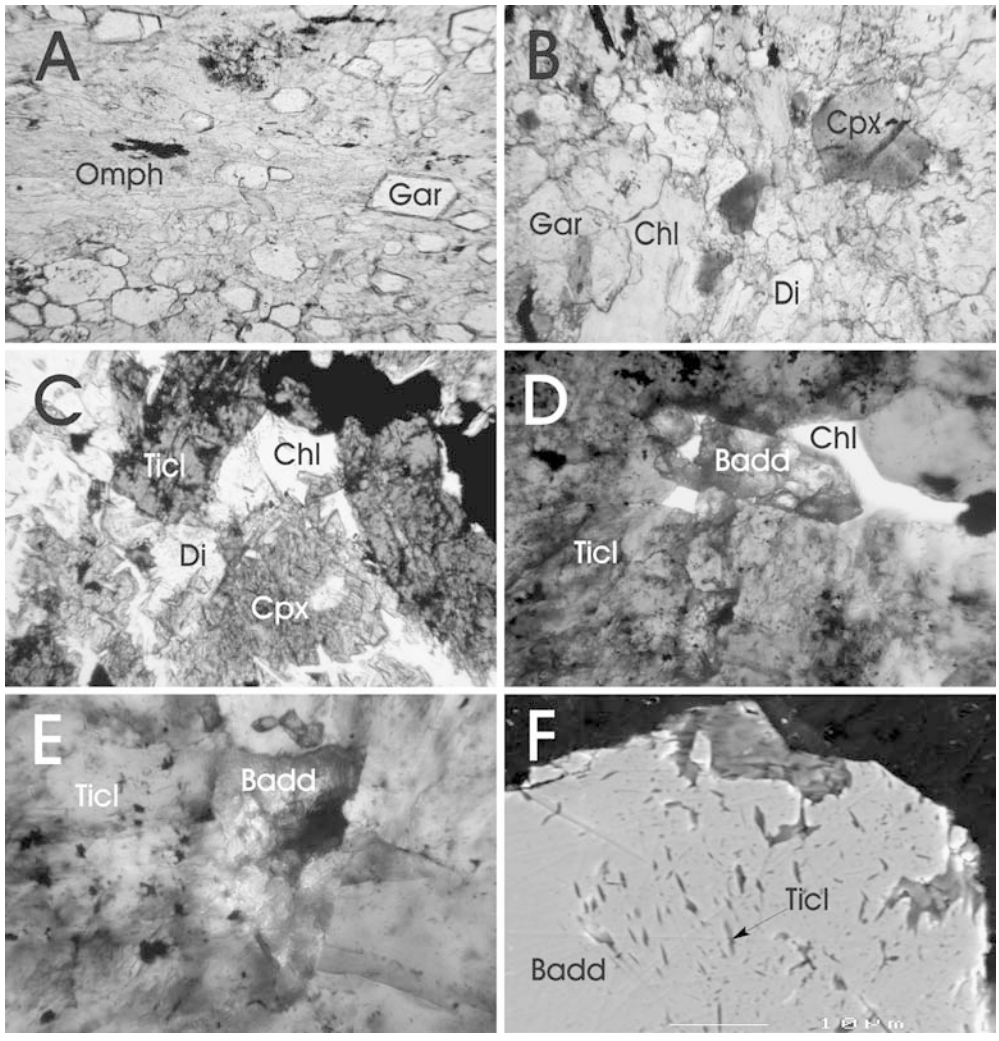

Fig. 2 **A** Beigua eclogite with omphacite (*Omph*) and garnet (*Gar*). **B** Beigua metarodingite with a grossular-rich garnet + chlorite (*Chl*) + diopside (*Di*) high-pressure assemblage. Also present are the relics of igneous, brown, Ti-augite (*Cpx*). **C** Ti-clinohumite dyke with a Ti-clinohumite (*Ticl*) + diopside + chlorite + magnetite HP assemblage. Still preserved are the relics of igneous Ti-augite. **D** Idiomorphic baddeleyite (*Badd*) included in Ti-clinohumite. Baddeleyite shows equilibrium relationships with the host high-pressure Ti-clinohumite and chlorite. **E** Enlargement showing the idiomorphic baddeleyite and its equilibrium boundaries with the Ti-clinohumite host. **F** Scanning electron microscope image of baddeleyite, showing microinclusions of Ti-clinohumite. Acicular Ti-clinohumite aggregates occur at the boundary of the baddeleyite crystal

Piampaludo area (Fig. 1b). The rims of the dyke are richer in Ti-clinohumite than the cores and are in contact with the surrounding olivine + antigorite-serpentinite (see Scambelluri and Rampone 1999 for a detailed description of the field relationships). The analysed samples contain Ti-clinohumite (up to 50% in rock volume), chlorite, diopside, magnetite, Ti-chondrodite, Ti-augite, ilmenite and apatite. Antigorite has been also observed within the HP paragenesis in contact with the clinohumite crystals.

The dykes frequently preserve the relics of igneous Ti-augite, ilmenite and apatite, which are evidence for a differentiated Fe-Ti-rich gabbroic protolith. Ti-augite is replaced along cracks, cleavages and in coronas by diopside + Ti-clinohumite (and Ti-chondrodite) + magnetite ±chlorite (Fig. 2C). Diopside also forms large individual crystals pseudomorphing the igneous Ti-augite in association with fine-grained Ti-clinohumite. Coarse corroded ilmenite is surrounded by large coronas of Ti-clinohumite, Ti-chondrodite and magnetite. Apatite is present in coarse patches of recrystallized grains and shows equilibrium textures with Ti-clinohumite, chlorite, diopside and magnetite forming the HP assemblage. Elsewhere, the dykes display replacement of Ti-clinohumite by retrograde neoblastic serpentine + ilmenite and formation of neoblastic chlorite. This mineral assemblage represents low-grade re-hydration of this rock type during a greenschist event, and such features were not observed in samples M1 and AF. This, together with the concomitant development of peak olivine + Ti-clinohumite in the associated serpentinites, indicates that in M1 and AF the Ti-clinohumite assemblage developed under peak, eclogite-facies, metamorphic conditions. The Ti-clinohumite dykes and the rodingites have thus been interpreted as the products of HP metamorphism of oceanic gabbros that respectively underwent pre-subduction Mg- and Ca-metasomatism as the result of exchanges with the host serpentinite (Scambelluri and Rampone 1999). The HP recrystallization presumably occurred at the same pressures and temperatures as the associated eclogites (Cimmino et al. 1981), i.e. 13 kbar and 450–500 °C.

The Ti-clinohumite and Ti-chondrodite aggregates can include millimetre-sized idiomorphic crystals of baddeleyite (Fig. 2D, E). In Fig. 2D, baddeleyite has

sharp and regular contacts with the surrounding clinohumite and chondrodite, as well as with chlorite patches included within the clinohumite aggregates. Scanning electron images of the baddeleyite crystals show the presence of micro-inclusions of the HP minerals Ti-clinohumite, diopside and chlorite. Ti-clinohumite in particular forms thin needle-like crystals and micro-aggregates within baddeleyite (Fig. 2F). Figures 2D, E and F document that baddeleyite both appears in textural equilibrium with the eclogite-facies minerals, and contains micro-inclusions of Ti-clinohumite and of other HP phases. Baddeleyite is therefore intergrown with these minerals and is interpreted to be part of the HP paragenesis.

Analytical techniques

Zircon and baddeleyite were prepared as mineral separates mounted in epoxy and polished down to expose the grain centres. Cathodoluminescence investigation of zircon was carried out at the Electron Microscope Unit, Australian National University, with a HITACHI S2250-N scanning electron microscope working at 15 kV, ~60 μA, and ~20 mm working distance.

Trace element analyses were performed by Laser Ablation – ICP-MS at the Research School of Earth Sciences (RSES) using a pulsed 193 nm ArF Excimer laser with 100 mJ energy at a repetition rate of 5 Hz, coupled to an Agilent 7500 quadrupole ICP-MS (Eggins et al. 1998). Laser sampling was performed in a He atmosphere using a 23 and 39 μm diameter spot size for zircon and 29 μm spot size for baddeleyite. Data acquisition was performed by peak hopping in pulse counting mode, acquiring individual intensity data for each element during each mass spectrometer sweep (ca. 1 s). A total of 85 sweeps, comprising a gas background of 25 sweeps, were performed for each analysis. During the time-resolved analysis, contamination from inclusions, fractures and zones of different composition was detected by monitoring several elements. A synthetic glass (NIST 612) was used as standard material. Internal standards were stoichiometric Si for zircon, and Hf for baddeleyite, measured by electron microprobe. Oxides, which are often the source of interference, were reduced to a minimum (ThO/Th $<0.4\%$) by ICP-MS tuning.

U-Th-Pb analyses were performed using a sensitive, high-resolution ion microprobe (SHRIMP II). Instrumental conditions and data acquisition were generally as described by Compston et al. (1992). The data were collected in sets of six or seven scans throughout the masses. The measured $^{206}Pb/^{238}U$ ratio was corrected using reference zircon from a gabbro of the Duluth Complex in Minnesota (AS3, 1,099 Ma, Paces and Miller 1993), whereas a zircon of known composition (SL 13) has been used to determine the U content of the target. For baddeleyite, the standard was Phalaborwa baddeleyite (2,060 Ma, Heaman and LeCheminant 1993). The data were corrected for common Pb on the basis of the measured $^{208}Pb/^{206}Pb$ (zircon) or $^{207}Pb/^{206}Pb$ (baddeleyite), as described in Compston et al. (1992). Owing to the young age and the low U content of the samples, some analyses have a high proportion of common Pb. However, in absolute amount, the common Pb content of the samples is similar to that of the common Pb-free standard. This indicates that the common Pb is mainly surface and instrumental background, the composition of which is known to be that of Broken Hill Pb ($^{204}Pb/^{206}Pb = 0.06250$, $^{207}Pb/^{206}Pb = 0.96180$, $^{208}Pb/^{206}Pb = 2.22850$). None of the mean ages calculated would change significantly if a different common Pb composition is used. Age calculations were done using the software Isoplot/Ex (Ludwig 2000). Isotopic ratios and single ages are reported with 1σ errors, whereas mean ages are at 95% confidence level.

Cathodoluminescence, U-Pb and trace element data

BVM metagabbro

Seventy zircon crystals were recovered from a 2-kg sample. They are pink, clear and rarely preserve crystal faces. Their size varies between 50 and 400 μm in length. In cathodoluminescence (Fig. 3a–c), most of the crystals show the broad-banded zoning usually observed in magmatic zircon from mafic rocks. Some have domains or rims with a weak cloudy zoning, often bright in cathodoluminescence (Fig. 3a).

The domains with magmatic zoning have a variable U and Th composition, with Th/U between 0.14 and 1.63 (Table 1). The analyses plot on or close to concordia (Fig. 4a) forming a well-sorted population with a mean $^{206}Pb/^{238}U$ age of 160 ± 1 Ma (95% c.l.; MSWD 0.96). The rims or cloudy-zoned domains are characterised by a very low U and Th content and a Th/U of 0.07–0.10. They yielded younger ages scattering between 152 and 32 Ma.

The zircon domains that display oscillatory zoning have a trace element composition (Table 2, Fig. 5a) similar to what reported for magmatic zircon in mafic rocks (Belousova et al. 2002; Rubatto 2002; Rubatto and Hermann 2003). They contain up to ca. 450 ppm P, and Hf in the order of 1.2–1.4 wt%. Y is another abundant trace element and its amount varies between ca. 1,500 and 3,700 ppm, similar to the HREE. Despite variations in absolute contents, the REE display parallel patterns. The chondrite-normalised patterns are characterised by a strong enrichment in HREE ($Lu_N/Sm_N = 102 \pm 15$), a pronounced positive Ce-anomaly and a negative Eu-anomaly ($Eu/Eu^* = 0.17 \pm 0.03$). The Ce-anomaly has been explained with the presence of Ce^{4+} in the rock (Hinton and Upton 1991), whereas the negative Eu-anomaly is interpreted to indicate zircon crystallization in the presence of a feldspar phase (Rubatto 2002), i.e. plagioclase in the protolith gabbro.

The domains or rims with irregular zoning have a trace element composition different from magmatic zircon (Table 2, Fig. 5a). They generally have lower concentrations than the magmatic domains of most of the trace elements. P and Y contents are reduced to half of that present in the oscillatory-zoned zircon (120–190 and 550–1,500 ppm, respectively). The depletion is particularly strong in the HREE, the content of which is a third of the magmatic domains. This is expressed in a reduced HREE enrichment with respect to MREE ($Lu_N/Sm_N = 29$–77). The positive Ce-anomaly and the negative Eu-anomaly ($Eu/Eu^* = 0.19 \pm 0.02$) are comparable with those observed in the other domains.

MF metarodingite

Zircon in the metarodingite is more abundant than in the metagabbro, with several hundreds of pink, clear

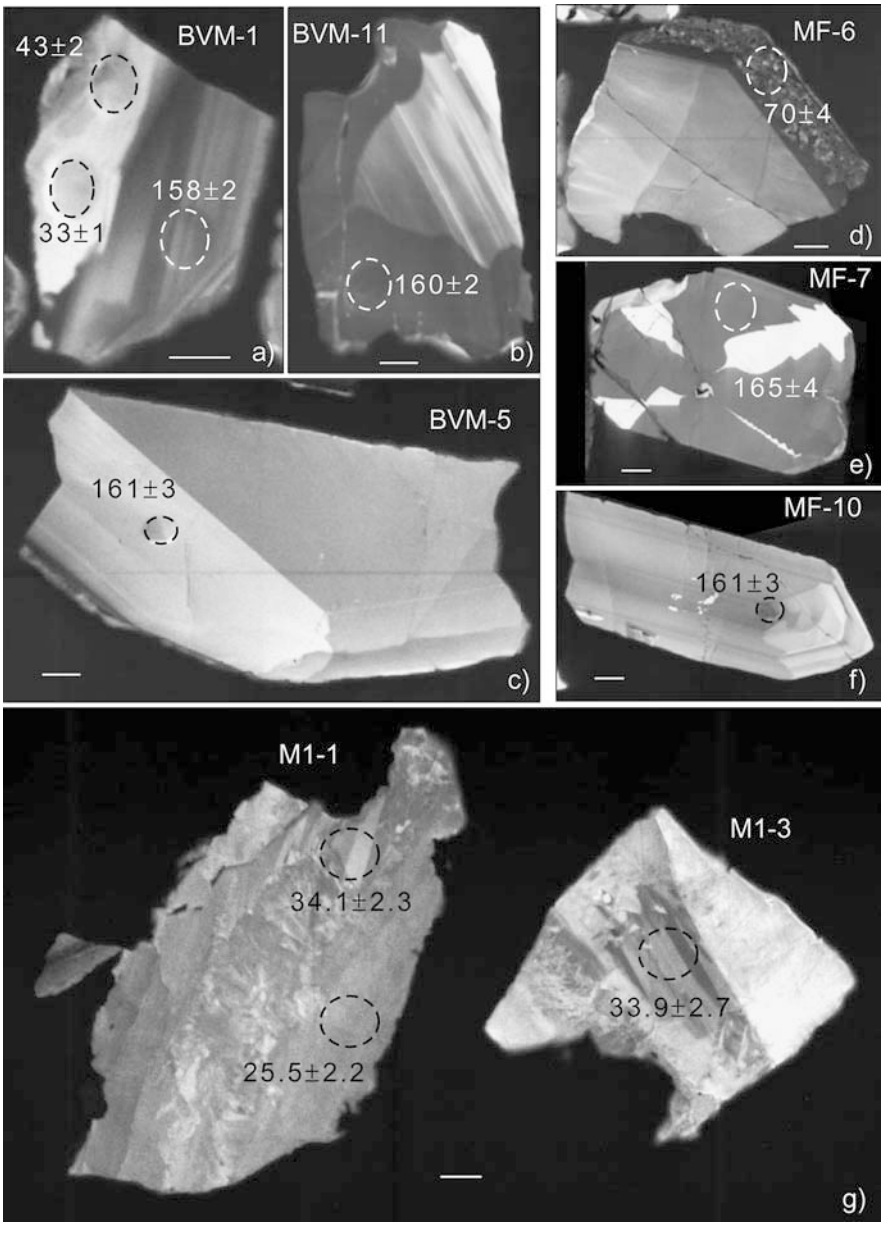

Fig. 3 Cathodoluminescence images of dated zircon crystals from metagabbro BVM (**a–c**), metarodingite MF (**d–f**), as well as baddeleyite crystals from Ti-clinohumite dyke M1 (**g**). *Numbers* represent $^{206}Pb/^{238}U$ ages $\pm 1\sigma$ in Ma. SHRIMP pits are marked with *circles*. In the zircon, ages younger than Jurassic are only found in rims lacking oscillatory, magmatic zoning (**a** and **d**). Scale bar represents 20 μm. See text for discussion

crystals in a 1.7-kg sample. The zircon crystals in this rock are bigger, with a diameter up to 1 mm and occasionally display euhedral shapes. The cathodoluminescence pattern is similar to the one of the zircon from the eclogitic metagabbro (Fig. 3d–f): magmatic, broad, oscillatory or sector zoning is prevalent in most crystals, and rare bright or cloudy-zoned domains are present along rims or fractures (Fig. 3d).

U and Th contents of the magmatically zoned crystals are systematically lower than in the metagabbro, and the Th/U is comparable (Table 1). The U-Pb analyses form a cluster close to the concordia with an average $^{206}Pb/^{238}U$ age of 161 ± 3 Ma (95% c.l.; MSWD 2.0; Fig. 4b). Opposite to what was observed in the other sample, the bright or cloudy-zoned domains are often richer in U and Th than the cores, and their Th/U is similar to the magmatic domains. Five of these domains analysed yielded apparent ages between ca. 132 and 69 Ma.

The zircon crystals with magmatic zoning from the metarodingite show a similar trace element composition to that of the zircon from the metagabbro, but with larger variations in absolute concentrations (Table 2, Fig. 5b). Their REE pattern has a similar trend to the metagabbro magmatic zircon with a strong enrichment in HREE with respect to MREE ($Lu_N/Sm_N = 100–300$) and a negative Eu-anomaly ($Eu/Eu^* = 0.30 \pm 0.05$). Because the non-zoned (i.e. non-magmatic) domains or rims are rare in these crystals, only two LA-ICPMS analyses were possible. Both analyses differ from the magmatic composition. The rim of crystal MV9 is richer in LREE than the magmatic domains, with MREE and HREE showing no significant variation from the magmatic zircon composition. The rim of crystal MV6 is

Table 1 U-Th-Pb SHRIMP analyses of zircon and baddeleyite. Errors on isotopic ratios and ages are at 1σ level

Zircon	U ppm	Th ppm	Th/U	$^{204}Pb/^{206}Pb$	% Pb com	$^{207}Pb/^{206}Pb$ $\pm 1\sigma$	$^{207}Pb/^{235}U$ $\pm 1\sigma$	$^{206}Pb/^{238}U$ $\pm 1\sigma$	Age $^{206}Pb/^{238}U$
BVM1.1[a]	38.2	2.7	0.07	0.01033	8.4	-	-	0.00505 ± 14	32.5 ± 1.1
BVM1.2	284.4	255.5	0.90	0.00034	0.4	0.0510 ± 10	0.1747 ± 40	0.02486 ± 28	158.3 ± 2.2
BVM1.3[a]	43.3	4.3	0.10	0.03058	12.7	0.0310 ± 95	0.0289 ± 89	0.00676 ± 18	43.4 ± 1.8
BVM2.1[a]	123.7	158.8	1.28	0.00014	1.2	0.0430 ± 16	0.1399 ± 58	0.02362 ± 36	150.5 ± 3.2
BVM3.1[a]	216.9	105.2	0.48	0.00048	0.5	0.0493 ± 12	0.1620 ± 43	0.02381 ± 28	151.7 ± 2.0
BVM4.1	154.1	249.7	1.62	0.00000	0.5	0.0627 ± 19	0.2177 ± 73	0.02518 ± 37	160.3 ± 3.4
BVM5.1	74.7	22.6	0.30	0.00173	1.2	0.0503 ± 22	0.1756 ± 82	0.02534 ± 38	161.3 ± 2.6
BVM6.1[a]	476.4	185.9	0.39	0.00099	0.4	0.0470 ± 8	0.1486 ± 31	0.02293 ± 25	146.2 ± 1.7
BVM7.1[a]	16.5	1.5	0.09	0.03752	14.3	-	0.0000 ± 0	0.00756 ± 28	48.6 ± 2.5
BVM8.1	882.6	679.5	0.77	0.00019	0.1	0.0508 ± 5	0.1804 ± 28	0.02573 ± 29	163.8 ± 2.1
BVM10.1[a]	6.5	0.5	0.07	0.02129	34.3	-	-	0.00393 ± 36	31.9 ± 4.2
BVM11.1	469.7	193.1	0.41	0.00036	0.2	0.0492 ± 8	0.1699 ± 32	0.02505 ± 27	159.5 ± 1.8
BVM12.1	175.2	93.0	0.53	0.00085	0.3	0.0477 ± 12	0.1687 ± 47	0.02568 ± 31	163.5 ± 2.2
BVM13.1	214.1	108.8	0.51	0.00035	0.3	0.0468 ± 11	0.1619 ± 44	0.02509 ± 30	159.8 ± 2.1
BVM20.1[a]	118.0	62.2	0.53	0.00267	0.6	0.0498 ± 19	0.1618 ± 67	0.02356 ± 39	150.1 ± 2.8
BVM21.1	141.6	88.4	0.62	0.00098	0.0	0.0570 ± 19	0.1927 ± 69	0.02451 ± 37	156.1 ± 2.6
BVM21.2[a]	180.5	116.6	0.65	0.00146	1.2	0.0437 ± 15	0.1415 ± 54	0.02346 ± 33	149.5 ± 2.5
BVM22.1	237.7	181.3	0.76	0.00000	0.0	0.0522 ± 15	0.1782 ± 56	0.02475 ± 33	157.6 ± 2.5
BVM23.1	657.2	873.9	1.33	0.00026	0.0	0.0555 ± 8	0.1920 ± 35	0.02508 ± 30	159.7 ± 2.4
BVM24.1	110.7	53.7	0.49	0.00123	1.0	0.0479 ± 19	0.1633 ± 70	0.02474 ± 39	157.6 ± 2.8
BVM25.1	167.1	87.1	0.52	0.00092	0.7	0.0489 ± 15	0.1683 ± 58	0.02495 ± 36	158.9 ± 2.5
BVM15.1	77.6	29.3	0.38	0.00000	0.1	0.0532 ± 23	0.1890 ± 88	0.02579 ± 45	164.1 ± 3.1
BVM16.1	264.4	141.4	0.53	0.00048	0.2	0.0484 ± 12	0.1656 ± 46	0.02482 ± 33	158.0 ± 2.3
BVM26.1	284.5	39.7	0.14	0.00022	0.2	0.0465 ± 12	0.1598 ± 47	0.02492 ± 32	158.7 ± 2.1
MF1.1	44.0	19.6	0.44	0.00000	2.1	0.0527 ± 32	0.1763 ± 109	0.02424 ± 44	154.4 ± 3.2
MF2.1[a]	401.1	486.9	1.21	0.00028	1.3	0.0419 ± 32	0.1085 ± 84	0.01879 ± 26	120.0 ± 2.3
MF3.1	94.6	63.4	0.67	0.00000	1.1	0.0467 ± 19	0.1572 ± 68	0.02438 ± 35	155.3 ± 2.6
MF5.1[a]	128.6	51.2	0.40	0.00047	1.2	0.0304 ± 23	0.0507 ± 39	0.01210 ± 18	77.6 ± 1.3
MF6.1[a]	1191.7	421.2	0.35	0.00024	0.5	0.0061 ± 7	0.0090 ± 12	0.01083 ± 54	69.4 ± 3.9
MF7.1	34.9	16.5	0.47	0.00276	0.9	–	0.1300 ± 190	0.02586 ± 50	164.6 ± 3.7
MF9.1[a]	45.5	19.5	0.43	0.00515	3.7	–	0.1352 ± 247	0.02062 ± 53	131.6 ± 3.3
MF9.2	76.1	31.8	0.42	0.00202	1.0	0.0513 ± 21	0.1792 ± 79	0.02536 ± 38	161.4 ± 2.7
MF10.1	224.0	463.9	2.07	0.00023	0.5	0.0595 ± 11	0.2071 ± 47	0.02523 ± 30	160.6 ± 3.1
MF11.1	33.2	23.8	0.72	0.00260	2.0	0.0547 ± 36	0.1830 ± 125	0.02425 ± 48	154.5 ± 3.7
MF2.2	63.5	29.4	0.46	0.00258	0.9	0.0583 ± 28	0.2056 ± 105	0.02560 ± 48	162.9 ± 3.4
MF12.1	25.3	9.6	0.38	0.00000	2.3	0.0542 ± 47	0.1915 ± 174	0.02561 ± 68	163.0 ± 4.8
MF13.1	50.7	18.7	0.37	0.00272	2.4	0.0414 ± 31	0.1495 ± 114	0.02622 ± 52	166.8 ± 3.7
MF14.1	91.0	78.3	0.86	0.00096	0.0	0.0565 ± 21	0.2070 ± 83	0.02658 ± 44	169.1 ± 3.4
MF15.1	96.9	74.3	0.77	0.00158	0.3	0.0502 ± 20	0.1785 ± 76	0.02576 ± 42	164.0 ± 3.2
MF16.1	91.8	121.9	1.33	0.00103	0.0	0.0660 ± 20	0.2439 ± 87	0.02682 ± 50	170.6 ± 4.9
MF17.1	139.6	88.2	0.63	0.00142	0.0	0.0561 ± 17	0.1976 ± 66	0.02554 ± 38	162.6 ± 2.7
MF18.1	84.7	25.3	0.30	0.00000	0.1	0.0527 ± 27	0.1791 ± 98	0.02466 ± 42	157.0 ± 2.8
MF19.1	55.1	62.7	1.14	0.00251	1.3	0.0462 ± 27	0.1568 ± 98	0.02462 ± 48	156.8 ± 4.1
MF20.1	94.8	58.5	0.62	0.00005	1.1	0.0444 ± 21	0.1536 ± 75	0.02507 ± 41	159.6 ± 3.0

Baddeleyite	U ppm	Th ppm	Th/U	$^{204}Pb/^{206}Pb$	% Pb com	Total $^{238}U/^{206}Pb$ $\pm 1\sigma$	Total $^{207}Pb/^{206}Pb$ $\pm 1\ \sigma$	Age $^{206}Pb/^{238}U$
M1-1.1	36.1	1.02	0.0283	0.02991	9.0	171.66 ± 10.57	0.1289 ± 227	34.1 ± 2.3
M1-2.1	109.0	0.01	0.0001	0.05385	5.6	187.18 ± 9.10	0.0979 ± 99	32.4 ± 1.6
M1-1.2[a]	25.9	0.07	0.0027	0.09538	16.3	210.99 ± 15.28	0.1953 ± 337	25.5 ± 2.2
M1-3.1	21.1	0.13	0.0063	0.00000	5.5	179.14 ± 12.74	0.0967 ± 288	33.9 ± 2.7
M1-4.1	53.8	8.58	0.1594	0.02787	20.6	159.25 ± 9.68	0.2348 ± 239	32.1 ± 2.4
M1-5.1	301.1	0.05	0.0002	0.00710	0.4	194.80 ± 4.13	0.0503 ± 41	32.9 ± 0.7
M1-6.1	41.8	10.45	0.2498	0.02518	22.1	165.77 ± 9.42	0.2488 ± 354	30.2 ± 2.5
M1-7.1	304.1	0.21	0.0007	0.00000	1.2	185.11 ± 3.93	0.0577 ± 45	34.3 ± 0.7
M1-9.1[a]	53.3	0.01	0.0001	0.00000	10.6	205.27 ± 10.66	0.1434 ± 208	28.0 ± 1.7
M1-10.1	112.8	0.04	0.0004	0.00000	4.1	178.09 ± 5.66	0.0847 ± 88	34.6 ± 1.2
AF1-1.1	88.6	0.07	0.0008	0.00000	11.1	182.81 ± 8.44	0.1483 ± 171	31.3 ± 1.6
AF1-2.1[a]	28.7	0.01	0.0004	0.06031	16.0	203.98 ± 13.70	0.1927 ± 302	26.5 ± 2.1
AF1-3.1	180.4	0.09	0.0005	0.01000	3.1	198.35 ± 5.29	0.0752 ± 68	31.4 ± 0.9
AF1-4.1	32.3	0.01	0.0002	0.04722	39.8	130.16 ± 6.72	0.4112 ± 376	29.7 ± 3.3
AF1-5.1	121.3	0.01	0.0001	0.01205	7.0	194.65 ± 6.67	0.1104 ± 112	30.7 ± 1.2
AF1-6.1	281.5	0.92	0.0033	0.00601	1.6	176.57 ± 3.59	0.0613 ± 40	35.8 ± 0.7
AF1-7.1	58.2	0.01	0.0002	0.00000	13.5	159.31 ± 6.88	0.1704 ± 175	34.9 ± 1.8
AF1-8.1[a]	86.8	0.01	0.0001	0.00000	10.6	237.67 ± 21.95	0.1436 ± 172	24.2 ± .3
M1-11.1	249.8	0.11	0.0004	0.00000	4.1	180.48 ± 4.59	0.0840 ± 76	34.2 ± 0.9

[a]Analysis not considered in the mean age calculation

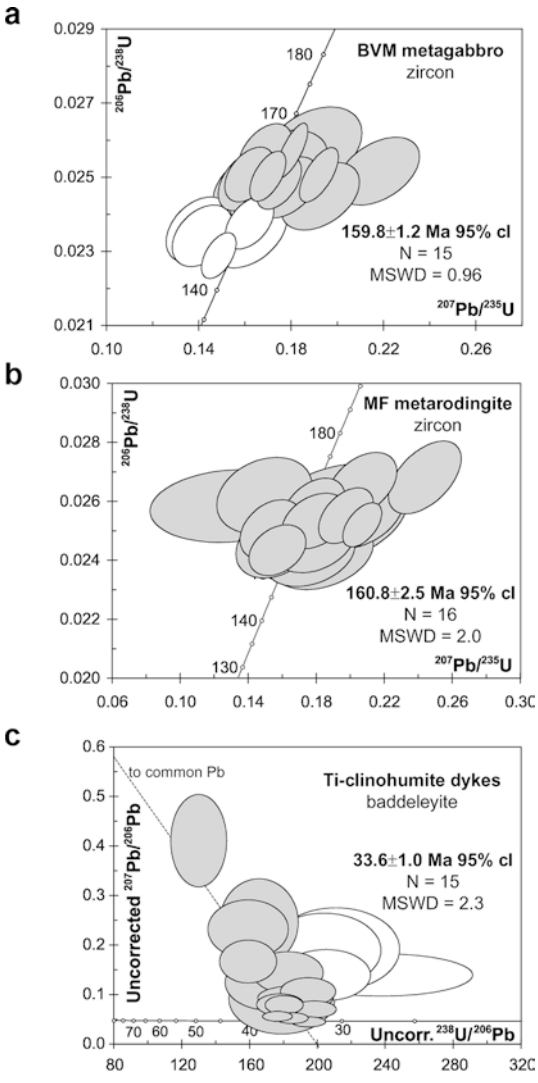

Fig. 4 U-Pb diagram representing analyses from zircon (**a** and **b**) and baddeleyite (**c**). *Ellipses* represent 2σ errors. *White ellipses* are excluded from the age calculation because of suspected Pb loss

richer in all trace elements with respect to the magmatic domains, with particularly high concentrations of U and Th, as already revealed by SHRIMP analysis.

Ti-clinohumite dykes

Several tens of baddeleyite crystals were recovered from the two relatively small samples of Ti-clinohumite dykes (ca. 1 kg). Both samples contain crystals or crystal fragments with irregular surface, which are pale brown to colourless, and transparent. A number of grains contain inclusions of metamorphic minerals such as chlorite, antigorite, diopside and Ti-clinohumite (Fig. 2F), trapped during crystallization of baddeleyite under HP conditions. The baddeleyite crystals have similar CL intensity as zircon. They display complex zoning patterns with areas in which oscillatory zoning is present and areas with a chaotic or cloudy zoning (Fig. 3g). The complex CL pattern was probably caused by a chaotic growth (or recrystallization) environment. Chaotic zoning is also common during sub-solidus growth of metamorphic zircon (e.g. Pidgeon 1992; Vavra et al. 1996; Pidgeon et al. 1998; Rubatto et al. 1998, 1999; Vavra et al. 1999): at these conditions, mineral growth and trace element influx are not constantly controlled by a melt, but may occur in episodes controlled by factors such as metamorphic reactions and deformation. Even more complex and chaotic would be recrystallization.

The isotope analyses were carried out on both oscillatory and cloudy areas, but no correlation between zoning pattern and age was found. Regardless of zoning pattern and U-Th content, most of the analyses yielded ages of 30–35 Ma, with the exception of four data points (M1–1.2, M1–9.1, AF1–2.1 and AF1–8.1; Table 1) that have younger apparent ages. The main cluster forms an array in the total $^{207}Pb/^{206}Pb$ versus total $^{238}U/^{206}Pb$ diagram along a regression line to common Pb (Fig. 4c). The intercept of this regression line defines a mean age of 33.6 ± 1.0 Ma. The high percent of common Pb in some of the analyses is due to low U content and thus low amount of radiogenic Pb in the baddeleyite (see analytical techniques for more details on common Pb correction). According to Wingate and Compston (2000), $^{206}Pb/^{238}U$ measured on baddeleyite can vary significantly with the relative orientation of the different crystals analysed, because of channelling of primary ions, emission of secondary ions along preferred directions and differential ionisation of secondary species. In our data set, however, nine analyses on the Phalaborwa standard yielded little scatter in $^{206}Pb/^{238}U$ (2σ error on the mean = 1.09) and a correct $^{207}Pb/^{206}Pb$ age ($2{,}058 \pm 11$ Ma). A good statistical fit was also found in the unknown (MSWD = 2.3). This suggests that the dispersion of Pb-U ratio in this data set is limited and the age of the samples is accurate.

Baddeleyite from both samples contains a significant amount of Hf (1.3–1.7 wt%), traces of Ti, Y, Nb, Ta, REE, U and Th (Table 2). The 17 analyses highlight large variability of the trace element composition that can span more than one order of magnitude between crystals. Part of this variability, particularly for the LREE, Nb and Ta, could be caused by micro-inclusions. To minimise this problem, only the part of the signal free of spikes was integrated for each analysis, but even then sub-micron inclusions cannot be avoided. In a number of analyses, zoning in some of the elements was observed. Despite the large variation, all the crystals analysed have a chondrite normalised REE pattern with enrichment in HREE with respect to the light and middle REE (Lu/Sm between 75 and 1,200) (Fig. 5c–d), which is similar to zircon. Common features are also the presence of a small negative Eu-anomaly and a positive Ce-anomaly. Both laser ablation and SHRIMP analyses indicate that baddeleyite has a medium to low U content and a very low Th content (2–250 and 0.011–10.4 ppm, respectively). The resulting low Th/U is in line with previous reports from magmatic

Table 2 Trace element analyses of zircon and baddeleyite obtained by LA-ICPMS

Zircon	BVM1C m	BVM13 m	BVM12 m	BVM8 m	BVM5 m	BVM15 m	BVM16 m	BVM9	BVM7	BVM1A	BVM1B	BVM10	MF10 m	MF11 m	MF9A m	MF7 m	MF6B m	MF6A	MF9B
P	353	293	462	448	237	333	324	145	190	175	160	123	292	399	775	574	855	2531	341
Y	1825	1970	3689	2980	1492	2455	2393	1353	1468	1133	1091	549	2225	1592	5119	1425	3999	12371	2074
Nb	0.891	0.248	0.323	0.610	0.263	0.241	0.402	1.867	0.537	0.600	0.755	0.266	0.339	0.364	1.02	0.336	1.67	10.2	0.591
La	< 0.078	< 0.078	< 0.078	< 0.078	< 0.078	< 0.078	< 0.078	< 0.078	< 0.078	< 0.078	< 0.078	< 0.078	< 0.078	< 0.078	< 0.078	< 0.078	0.958	1.07	4.84
Ce	9.40	4.72	7.25	12.5	2.89	5.19	5.32	7.60	6.26	6.50	6.73	1.74	2.08	2.93	12.3	1.68	23.2	75.1	10.8
Pr	< 0.065	0.102	0.271	0.210	0.088	0.171	0.173	0.111	0.105	< 0.065	< 0.065	< 0.065	0.100	< 0.065	0.227	< 0.065	0.719	1.87	1.64
Nd	1.11	2.43	4.95	3.99	2.03	3.45	3.07	2.60	2.77	1.21	0.925	0.787	2.52	1.18	5.41	0.66	8.25	25.7	13.7
Sm	3.45	5.10	9.13	8.42	4.50	7.02	6.46	6.15	5.93	3.37	3.53	1.87	6.00	3.26	12.6	2.07	10.3	25.5	8.20
Eu	0.847	0.961	1.78	1.13	1.03	1.35	1.29	1.17	1.32	0.867	0.927	0.367	2.18	1.17	3.15	0.92	3.96	4.76	2.52
Gd	28.8	34.9	65.8	56.8	27.9	47.4	43.1	39.8	34.5	29.7	29.9	11.5	42.4	23.5	85.1	17.9	62.8	176	39.5
Tb	11.0	12.3	23.4	19.3	9.48	16.3	15.1	12.5	11.6	10.2	10.1	3.81	15.2	9.03	31.6	7.27	22.0	73.3	13.0
Dy	160	172	327	267	132	224	212	153	148	130	127	51.7	214	139	469	118	334	1112	188
Ho	56.4	60.4	114	90.1	46.1	76.1	73.4	42.0	45.0	39.5	37.4	17.1	72.0	50.2	169	45.5	125	395	67.0
Er	250	281	517	400	215	342	339	154	174	151	139	75.5	318	241	811	232	623	1874	324
Tm	52.1	60.7	109	80.7	46.9	71.5	71.7	27.1	31.8	30.0	26.9	16.1	67.1	54.1	179	55.4	144	423	73.4
Yb	399	486	857	608	386	566	571	185	217	231	212	128	542	455	1500	499	1249	3581	635
Lu	70.8	90.8	160.6	106.2	76.8	104.4	107.5	29.4	33.9	40.5	38.8	23.7	101	87.1	295	103	249	701	131
Hf	9727	11505	10803	14408	9797	10837	11326	8677	13108	11052	11270	11008	13252	6399	11520	5414	17300	29102	11321
Ta	1.043	0.110	0.133	0.601	0.093	0.104	0.144	3.913	0.927	0.688	0.687	< 0.179	0.226	0.131	0.493	0.129	1.28	11.3	0.217
Th	170	66.4	139	478	25.1	75.6	85.5	79.2	79.1	92.6	46.6	15.2	90.2	52.9	37.3	7.01	60.4	1680	16.0
U	190	135	236	756	52.7	144	166	47.4	131	111	101	37.7	52.4	55.3	77.3	21.2	143	1618	37.9
Th/U	0.90	0.49	0.59	0.63	0.48	0.52	0.51	1.67	0.60	0.84	0.46	0.40	1.72	0.96	0.48	0.33	0.42	1.04	0.42
Eu/Eu*	0.18	0.16	0.16	0.12	0.22	0.17	0.18	0.17	0.22	0.18	0.19	0.19	0.31	0.30	0.22	0.32	0.37	0.16	0.35
LuN/SmN	125	109	108	77	104	91	102	29	35	73	67	77	103	163	143	304	149	168	98
Baddeleyite	M1-1	M1-3	M1-4	M1-6	M1-8	M1-9	M1-10	M1-15	M1-17	AF1-0	AF1-2	AF1-1	AF1-3	AF1-4	AF1-10	AF1-11	AF1-12		
Ti	190	502	500	417	59.5	101	127	550	137	441	52.8	174	122	82.4	946	58.0	76.8		
Y	60.0	268	171	166	28.1	69.6	101	50.9	69.8	195	14.2	316	91.2	71.3	833	10.2	38.9		
Nb	0.610	0.686	0.736	0.732	6.72	28.9	20.7	1.63	0.505	1.20	12.2	20.7	39.5	11.0	1.11	0.406	0.335		
La	0.238	0.061	1.86	1.09	0.040	bdl	bdl	bdl	0.058	3.12	bdl	bdl	bdl	0.019	0.118	0.099	0.090		
Ce	1.78	5.43	10.6	8.26	0.162	0.140	0.595	0.665	0.433	12.4	0.065	1.09	0.745	0.305	20.1	0.386	0.536		
Pr	0.158	0.071	0.922	0.577	0.016	bdl	0.009	bdl	0.042	1.37	0.012	bdl	bdl	0.025	0.207	0.063	0.066		
Nd	0.578	0.676	4.80	3.91	bdl	bdl	0.093	bdl	0.105	7.08	bdl	0.089	0.084	0.166	1.93	0.204	0.436		
Sm	0.230	0.667	2.11	1.77	0.079	bdl	0.111	0.066	0.219	2.87	0.116	0.294	bdl	bdl	2.94	0.115	bdl		
Eu	0.172	0.511	0.856	0.786	0.027	0.042	0.102	0.054	0.065	1.15	0.021	0.346	0.087	0.026	1.93	0.027	0.047		
Gd	1.06	3.26	4.75	3.97	0.288	0.541	0.891	0.404	0.796	5.49	bdl	2.67	0.715	0.417	12.9	bdl	0.381		
Tb	0.442	1.57	1.61	1.42	0.111	0.344	0.568	0.281	0.409	1.89	0.045	1.77	0.418	0.322	6.09	0.056	0.217		
Dy	6.87	27.8	20.7	20.4	2.63	6.73	9.83	5.17	7.42	25.7	1.06	32.5	9.11	6.43	96.0	0.938	3.93		
Ho	2.99	12.1	7.68	7.56	1.35	3.33	4.82	2.63	3.42	9.40	0.72	14.79	4.50	3.41	38.6	0.565	1.80		
Er	16.7	80.2	43.2	43.3	10.1	24.9	31.4	17.5	21.8	49.2	5.56	96.5	30.7	23.3	218	3.29	11.6		
Tm	4.52	22.8	11.7	11.9	3.39	8.44	10.0	5.58	6.28	12.5	2.16	27.7	9.57	8.27	57.5	1.26	3.56		
Yb	49.8	266	128	139	34.0	94.5	104	66.7	73.1	127	24.2	257	95.2	86.7	593	18.9	42.8		
Lu	9.32	57.8	25.7	27.8	4.13	13.0	13.6	13.1	14.9	21.0	3.58	34.1	12.1	12.2	99.7	3.80	8.64		
Hf	12875	11295	13158	13675	14349	13651	13315	11380	11455	12085	14326	13881	11685	11694	11593	12281	12051		
Ta	0.215	0.198	0.263	0.278	2.13	11.0	6.34	0.319	0.131	0.288	3.82	6.30	12.1	5.16	0.290	0.130	0.104		
Th	0.421	1.75	8.18	9.15	bdl	bdl	0.058	0.022	0.054	1.87	bdl	0.065	0.064	0.011	6.14	bdl	0.108		
U	22.0	13.1	75.1	77.0	19.1	40.2	137	13.9	3.05	14.012	17.030	162.782	178.075	83.003	21.020	1.991	2.969		
Th/U	0.019	0.134	0.109	0.119	–	–	0.000	0.002	0.018	0.133	–	0.0004	0.0004	0.0001	0.292	–	–		
Eu/Eu*	0.89	0.87	0.80	0.88	0.49	–	0.70	0.78	0.43	0.88	–	0.80	–	–	0.81	–	–		
LuN/SmN	248	530	74	96	319	–	752	1216	417	45	188	711	–	–	207	202	–		

m Domain preserving a magmatic age; *bdl* below detection limit; *LuN*/*SmN* ratio normalised to chondrite values

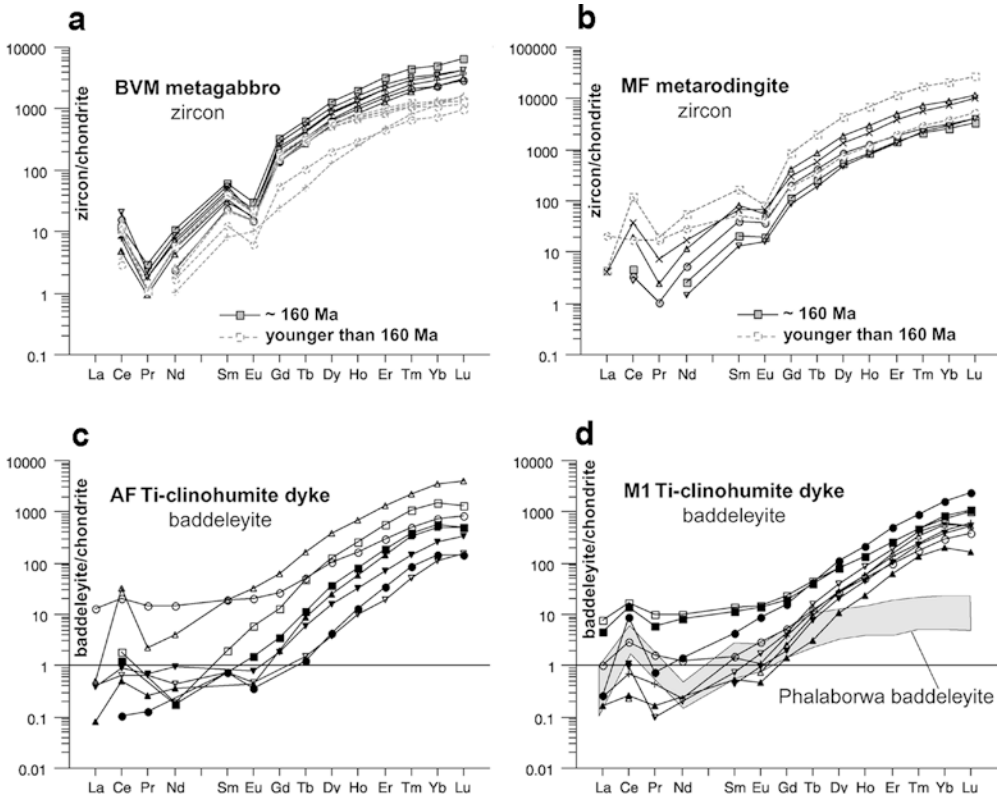

Fig. 5 Chondrite normalised REE patterns for zircon (**a** and **b**) and baddeleyite (**c** and **d**). See text for discussion

and metamorphic baddeleyite (Heaman and LeCheminant 1993; Reischmann et al. 1995; Wingate and Compston 2000), and confirms the strong Th-U fractionation in this mineral.

The only available trace element study of baddeleyite from similar rocks is reported by Stucki et al. (2001). They analysed baddeleyite from metarodingites derived from Fe-Ti gabbros in the Central Alps (Bellinzona-Dascio Zone), but they could not determine the origin (magmatic vs. metamorphic) of the baddeleyite. The analyses of Stucki et al. (2001) also showed a REE pattern with enrichment in HREE with respect to the light and middle REE, but a much higher trace element content and hardly any Ce- or Eu-anomaly. These differences are most probably due to the environment (whole rock composition, Ce oxidation state and possibly absence of plagioclase) in which that baddeleyite formed.

Previous analyses of baddeleyite from the Phalaborwa carbonatite (Reischmann et al. 1995) obtained with various techniques (microprobe, neutron activation, spark source and thermal ionisation mass spectrometry) resulted in an unusual "U" shaped REE pattern, with no Eu-anomaly. Six analyses of the Phalaborwa baddeleyite (used as the U-Pb standard during SHRIMP measurements) performed during the same analytical session of the Beigua baddeleyite, yielded values for Nb, Th and the REE lighter than Gd that are lower than those reported by Reischmann et al. (1995). According to our data, the Phalaborwa baddeleyite have a REE pattern similar to the Beigua ones (Fig. 5d), but at lower trace element contents, particularly the HREE, as expected in carbonatite. It is therefore possible that the analyses of Reischmann et al. (1995) were compromised by inclusions and impurities in the separate.

Discussion

Magmatic zircon: Jurassic ophiolite formation

From our petrographic investigation we conclude that despite a dominant eclogite-facies overprint, the analysed samples still retain the relics of primary igneous minerals such as clinopyroxene, apatite and oxides. The metagabbro and the metarodingite both preserve zircon crystals with oscillatory or sector zoning, representing strong indication of their primary igneous origin. Their medium Th/U, their average U and Th content and, in particular, their REE patterns are typical for magmatic zircon equilibrated with a plagioclase-bearing igneous assemblage. The age of these domains is thus interpreted as dating the intrusion of the gabbroic protoliths at 160 ± 1 and 161 ± 3 Ma.

The igneous crystallization age of the Beigua metagabbros is similar to that obtained for other ophiolitic gabbros throughout the Western Alps and Northern Apennines: Zermatt–Saas Fee (164 ± 3 Ma, Rubatto et al. 1998), Gets Nappe in the Prealps (166 ± 1 Ma, Bill et al. 1997), Monviso (163 ± 2 Ma, Rubatto and Hermann 2003), Internal Ligurides (164 ± 14 Ma, Rampone et al. 1998) and External Ligurides (165 ± 20 Ma,

Rampone et al. 1995). This age is older than the U-Pb ages of ca. 156 and ca. 150–153 Ma obtained for Fe-diorites and plagiogranites, respectively, of the Voltri Group and Northern Apennines (Borsi et al. 1996), which represent the late-stage intrusion of highly differentiated melts within the Tethyan oceanic crust (e.g. Lombardo et al. 2002). The data also confirms the hypothesis that Alpine and northern Apennines ophiolite formed in a relatively short period of time.

Metamorphic baddeleyite

Baddeleyite in terrestrial samples is most commonly found in mafic intrusive rock suites as an accessory mineral within the late, highly differentiated melts (Heaman and LeCheminant 1993). During regional metamorphism, magmatic baddeleyite is often substituted or overgrown by metamorphic zircon because of increased silica activity (e.g. Davidson and van Breemen 1988). Purtscheller and Tessadri (1985) reported baddeleyite rimmed by zirconolite in polymetamorphic carbonates that underwent contact metamorphism. These authors could not determine the origin of the baddeleyite. Similarly, baddeleyite has been documented in a metarodingite in the Central Alps, but its metamorphic origin has not been proven and it could represent a magmatic relict (Stucki et al. 2001). Therefore, no previous unequivocal report of baddeleyite formed during metamorphism exists. It is thus important to understand when the baddeleyite formed in the investigated samples, and how it reacted to metamorphism.

The analysed baddeleyite-bearing Ti-clinohumite dykes derive from highly differentiated gabbroic precursors, which underwent metasomatic alteration and which might have contained baddeleyite and/or zircon in the primary igneous assemblage. However, the age of baddeleyite and its inclusions of metamorphic minerals indicate its metamorphic (re)crystallization. Moreover, the baddeleyite has only a small negative Eu-anomaly, which is in line with metamorphic formation in the absence of feldspars, as already documented for eclogite-facies zircon (Rubatto 2002; Rubatto and Hermann 2003). Like zircon, magmatic baddeleyite crystallized in a gabbroic rock is expected to have a marked Eu-anomaly because of coeval crystallization of plagioclase. Baddeleyite might have formed at eclogite-facies conditions from the breakdown of a Zr-bearing mineral, such as magmatic clinopyroxene or zircon. The relics of magmatic pyroxene preserved in the dykes contain 49 ppm Zr, whereas the whole rock contains 189 ppm Zr (Scambelluri and Rampone 1999). No other major magmatic mineral is expected to host a significant amount of Zr. The chemical data indicate that clinopyroxene was not the only Zr repository in these rocks, and that zircon or baddeleyite were likely part of the igneous assemblage. If magmatic zircon was present, it probably did not survive the oceanic metasomatism that involved Mg-enrichment and strong Si-depletion (Cimmino et al. 1979; Scambelluri and Rampone 1999). This type of metasomatism is the prime candidate for silica loss and might have been responsible for baddeleyite formation at the expense of the pre-existing magmatic zircon. Scambelluri and Rampone (1999) argued that this metasomatic event occurred in the oceanic environment, during the Jurassic. Baddeleyite might therefore have been present in the Ti-clinohumite dykes long before Alpine HP metamorphism, either as igneous phase or as metasomatic product. However, baddeleyite in both samples contains inclusions of eclogite-facies minerals, and no remnants of pre-Alpine baddeleyite were found during the isotopic analyses. Additionally, the different baddeleyite crystals have trace element composition variable in absolute amounts, but similar in pattern. These observations indicate that the sample contains a single generation of baddeleyite formed during Alpine metamorphism. This implies that any pre-subduction baddeleyite, either magmatic or metasomatic, was completely recrystallized or dissolved and re-precipitated during Alpine metamorphism, with consequent chemical and isotopic re-equilibration.

Compared to zircon, this response to metamorphism is unusual. Recrystallization and crystallization of zircon in rocks that underwent metamorphism below 600–700 °C is rare. At these conditions, zircon dissolution and precipitation may take place in presence of excess fluids in metamorphic veins (Liati and Gebauer 1999; Rubatto et al. 1999; Rubatto and Hermann 2003). More commonly, zircon partly recrystallizes along grain boundaries or fractures to form rims or domains yielding the age of metamorphism or a mixing age (e.g. Pidgeon 1992; Vavra et al. 1996; Pidgeon et al. 1998; Rubatto et al. 1998; Rubatto et al. 1999; Vavra et al. 1999; Hoskin and Black 2000). This suggests that baddeleyite might be more reactive to low temperature-HP metamorphism than its close relative zircon.

Early Oligocene high-pressure metamorphism

The zircon domains or rims lacking oscillatory zoning display the same characteristics in the metagabbro and the metarodingite. They have a trace element composition differing from magmatic zircon and yield younger ages. Depletion in trace elements, decrease in Th/U and variation in REE patterns have been previously described for zircon formed or recrystallized at sub-solidus conditions (Pidgeon 1992; Hoskin and Black 2000; Rubatto 2002). During this process, migration of trace elements and loss of radiogenic Pb also occur. Recrystallization and chemical resetting in zircon can be incomplete (Pidgeon 1992), thus leading to mixed ages. Pb loss can occur at low temperatures because of fluid leaching along fractures. In the metagabbro, the zircon domains yielding an apparent young age systematically have low U content and low Th/U, in line with partial age resetting by recrystallization or leaching during Alpine metamorphism, or more recently. Additionally,

some of the analyses yielding young ages have a high proportion of common Pb (up to 34%), suggesting possible analytical problems such as low U content, excessive surface contamination and sampling of Pb-rich inclusions or fractures. Finally, these analyses are mostly discordant and do not cluster. For all the above reasons, the apparent ages between ca. 132 and ca. 32 Ma are considered geologically meaningless. It is relevant that, despite the pervasive eclogite-facies recrystallization, particularly in the eclogitic metagabbro, only a small proportion of the magmatic zircon show signs of metamorphic overprint in the form of partly recrystallized domains.

The baddeleyite in the Ti-clinohumite dykes dates an Alpine event at 33.6 ± 1.0 Ma. The analysed baddeleyite crystals were recovered from samples that preserve a fresh HP assemblage and display very little retrogression. Idiomorphic baddeleyite is mainly included in the HP Ti-clinohumite and chondrodite, it is in textural equilibrium with the other HP phases and contains inclusions of the HP minerals Ti-clinohumite, chlorite, antigorite and diopside. It is thus concluded that the baddeleyite is intergrown with the HP minerals and therefore formed during eclogite-facies metamorphism. Because baddeleyite, like zircon, does not experience significant by diffusion Pb loss at geological temperatures (Davidson and van Breemen 1988; Heaman and LeCheminant 1993), and certainly not at 450–500 °C, its age is interpreted as formation age dating HP metamorphism at 33.6 ± 1.0 Ma. We cannot, however, fully exclude the possibility that the baddeleyite re-equilibrated at lower pressures during uplift, given that the rock HP paragenesis could be stable during the early stages of exhumation, at pressures compatible with blueschist facies. We can claim however that the 33.6 ± 1.0 Ma age does not correspond to greenschist-facies metamorphism, since at these conditions high-pressure Ti-clinohumite undergoes re-hydration to serpentine + ilmenite. These retrograde effects are absent in the analysed samples, where the HP mineral phases are well preserved both as rock-forming minerals and as micro-inclusions in baddeleyite. We therefore rate the retrograde re-equilibration of baddeleyite as an unlikely possibility, because we have textural indication that the rock mineral assemblage is of HP (see sample description). The country rocks also preserve the peak HP paragenesis (olivine overgrowing prograde antigorite, Cimmino et al. 1981; Scambelluri and Rampone 1999) with no significant retrogression. Signs of limited isotopic disturbance post-dating the metamorphic peak might be seen in the four analyses younger than 33 Ma (Fig. 4c). These analyses correspond to crystal borders and probably lost Pb because of fluid leaching along fracture and grain boundaries. This led to partial resetting of their apparent U-Pb age.

An Oligocene age for the HP metamorphism in the Voltri Massif is somehow surprising and needs to be discussed in light of the formation ages of the Tertiary sedimentary sequences which overly the HP Voltri terrains, as well as of the ages of other high- to ultra-high-pressure rocks of the Western Alps. In the Voltri Massif and in other Alpine high-pressure terrains, pre-Oligocene and possibly pre-Late Eocene exhumation of eclogites has been proposed so far, based on the occurrence of eclogitic pebbles in the Late Eocene to Oligocene clastic deposits of the Tertiary Piemontese Basin (discussion in Spalla et al. 1996). The age of 33.6 ± 1.0 Ma for HP metamorphism in the Beigua unit is extremely close to the age of the overlaying sediments of the Tertiary Piemontese Basin. The lowermost portions of such a sedimentary sequence are constituted by the coarse grained deposits of the Costa Cravara Breccia, which has been taken to mark the surface exposure of the HP Alpine units (Cortesogno and Haccard 1984). This breccia was indirectly dated at the Late Eocene, since it is overlain by Early Oligocene conglomerate deposits (Pianfolco and Molare Formations, Charrier et al. 1964; Gelati et al. 1998). However, on a biostratigraphic basis, Gelati et al. (1993) suggested that the boundary between the basal conglomeratic level and the overlaying sandstone is 30 Ma old (Late Oligocene). Di Biase et al. (2002) have recently documented that HP pebbles do not appear in these sequences until the Lower Oligocene. Based on biostratigraphic evidence, Di Biase and Pandolfi (1999) have, moreover, proposed a later formation age for the Cravara Breccia, Pianfolco and Molare formations (between 32 and 30 Ma, Pandolfi, personal communication), after complete exhumation and tectonic unroofing of the nearby HP terrains. This new hypothesis implies that after eclogite-facies metamorphism at 33.6 ± 1.0 Ma, the Beigua Unit might have been exhumed and partly eroded between 30 and 32 Ma.

Tectonic implications

The exhumation rates required by the above scenarios are extremely fast, but not unusual for the Alpine high- to ultra-high-pressure rocks. In fact, in the Dora Maira ultra-HP unit, which crops out 100 km to the west (Fig. 1a), the initial stage of exhumation from 120 km depth proceeded at a rate as high as 3.6 cm/year, then slowing to 0.5 cm/year at upper crustal levels (Rubatto and Hermann 2001). In order to exhume the Beigua Unit in 2 m.y. from depths of about 40–50 km (pressure estimates in Messiga and Scambelluri 1991; Liou et al. 1998), an average rate of 2.5 cm/year is required. Following the example of the Dora Maira, this probably implies even faster uplift in the initial stage and slower exhumation when the unit is involved in nappe stacking. The intense degree of serpentinisation, the stability of serpentine in this unit at eclogite-facies and, consequently, its extremely low-density, is interpreted to have played an important role for its prompt, buoyant return towards the surface (Scambelluri et al. 1995; Hermann et al. 2000) in a short period of time.

According to several geochronological studies applying different methods, the other HP ophiolite complexes of the Alps (e.g. Zermatt-Saas and Monviso, Fig. 1a) formed in the Jurassic and underwent Eocene subduction at around 45 Ma (Dûchene et al. 1997; Rubatto et al. 1998; Rubatto and Hermann 2003). An exception is the Chiavenna unit in the Central Alps, which formed in the Cretaceous (ca. 93 Ma Liati et al. 2003) as part of the Valais ocean and not the Tethys ocean, to which all the other ophiolites discussed here belong. The Chiavenna unit underwent metamorphism in the Late Eocene (37.1 ± 0.9 Ma Liati et al. 2003). The ages of HP metamorphism in these Alpine ophiolites appear intermediate between the 65 to 69 Ma recorded by the subducted Adriatic margin (e.g. Sesia-Lanzo Zone Inger et al. 1996; Dûchene et al. 1997; Rubatto et al. 1999), and the 35–32.8 Ma attributed to the subducted slices of the European plate, such as the Monte Rosa and Dora Maira (Dûchene et al. 1997; Gebauer et al. 1997; Rubatto and Gebauer 1999; Rubatto and Hermann 2001). This trend of southward younger ages has been suggested to reflect transition from subduction of the Adriatic margin, to the Tethys Ocean ($\sim$45 Ma), to subduction of the European continental margin followed by continental collision (Rubatto et al. 1998; Liati et al. 2003). However, the HP age of the Beigua rocks is significantly younger than that of most Alpine ophiolites and overlaps with peak metamorphic age of units that represent the European continental margin. The finding of subduction of oceanic crust at 33.6 ± 1.0 Ma shows that the tectonic scenario must be more complex.

Several possibilities can be taken to explain such an Early Oligocene age for the Voltri HP metamorphism. Considering the general scenario with subduction progressing from the Adriatic to the European margin, the Beigua ophiolite could have been a marginal part of the oceanic realm very close to the European continental margin. It is also possible that the Beigua ophiolite was an oceanic slice in a similar position to Zermatt-Saas or Monviso which, before subduction and exhumation, resided for several million years at the upper levels of the subduction wedge. Oblique subduction with units to the south, i.e. the Beigua Unit, being subducted later than others in the north is another feasible scenario. In fact, compression in the Apennine region, south of the Voltri massif, progressively migrated from Oligocene to present (Brunet et al. 2000) and thus occurred later than in the Alps. As an alternative, the difference in ages of the various Alpine ophiolites and other HP slices may be unrelated to a pre-subduction paleogeographic setting (Polino et al. 1990), but rather be the result of tectonic erosion and indentation of oceanic and continental slices at the onset of subduction. In this case the 65, 45 and 35 Ma ages in Alpine eclogites, particularly the range in age recorded by the ophiolite slices, may not be the product of progressing subduction (see Rubatto et al. 1998), but may simply reflect the episodic tectonic regurgitation of the deeply accreted buoyant material.

Conclusions

Zircon was found in eclogite-facies metagabbro and metarodingite derived from Fe-Ti-rich gabbros within the Beigua Unit. The crystals are recognised as magmatic relics on the basis of their oscillatory and sector zoning and their chemical composition: medium Th/U, average U and Th contents and in particular REE patterns strongly enriched in HREE and with negative Eu-anomaly. The U-Pb ages obtained from the two samples (160 ± 1 and 161 ± 3 Ma, respectively) are interpreted as dating the crystallization of the protolith gabbros. These ages are similar to those determined for other Alpine and Apennine ophiolites and support the hypothesis that the Tethys ocean formed in a relatively short period of time (160–165 Ma).

Euhedral baddeleyite crystals are contained in Ti-clinohumite dykes of the same unit. The textural relationships with HP minerals, the trace element composition and the age constraint indicate that this baddeleyite is metamorphic. According to petrological data, the baddeleyite (re)crystallized during HP metamorphism from magmatic or metasomatic pre-existing zircon or baddeleyite. This first finding of eclogite-facies baddeleyite suggests that this mineral might be more reactive to low temperature – HP metamorphism than its close relative zircon.

The age of 33.6 ± 1.0 Ma determined on selected baddeleyite domains is interpreted as constraining the eclogite-facies metamorphism of the Beigua Unit to the Early Oligocene. Since the continental sediments overlying the Voltri massif containing pebbles of HP rocks are dated at 30–32 Ma, there is direct evidence that the exhumation of the Beigua Unit was extremely fast and likely occurred in a couple of million years.

The age of the Beigua eclogites is surprisingly young when compared to the Alpine HP units and, in particular, it is more than 10 Ma younger than HP metamorphism in other oceanic units of the Western Alps. This age, so far known only for the subduction of continental crust of the European margin (Dora Maira and Monte Rosa), suggests new possible scenarios for the progression of Alpine subduction. The Beigua ophiolite was located in proximity of the European margin and was subducted later than the other ophiolite massifs attributed to the Tethys oceanic basin. Alternatively, the Beigua Unit possibly resided for a several million years at the upper levels of the wedge before subduction. A third alternative is that Alpine subduction did not proceed according to paleogeographic location of the units, but is the result of chaotic tectonic erosion and indentation of oceanic and continental slices in the subduction plane. Their fast return to the surface may then depend on episodic tectonic regurgitation of deeply accreted buoyant materials.

Acknowledgements We thank the Electron Microscope Unit at the Australian National University for access to the SEM facilities. Charlotte Allen, Steve Eggins and Mike Shelley kindly assisted with

the LA-ICP-MS analysis. This work has benefited from discussion with J. Hermann, R. Polino and L. Pandolfi. Comments from A. Möller and an anonymous reviewer improved the manuscript.

References

Agard P, Monié P, Jolivet L, Goffé B (2002) Exhumation of the Schistes Lustrés complex: in situ laser probe $^{40}Ar/^{39}Ar$ constraints and implications for the Western Alps. J Metamorph Geol 20:599–618

Belousova EA, Griffin WL, O'Reilly SY, Fisher NI (2002) Igneous zircon, trace element composition as an indicator of source rock type. Contrib Mineral Petrol 143:602–622

Bill M, Bussy F, Cosca M, Masson H, Hunziker JC (1997) High-precision U-Pb and $^{40}Ar/^{39}Ar$ dating of an Alpine ophiolite (Gets nappe, France). Eclogae Geol Helv 90:43–54

Borsi L, Schärer U, Gaggero L, Crispini L (1996) Age, origin and geodynamic significance of plagiogranites in lherzolites and gabbros of the Piedmont-Ligurian ocean basin. Earth Planet Sci Lett 140:227–241

Brunet C, Monié P, Jolivet L, Cadet J-P (2000) Migration of compression and extension in the Tyrrhenian Sea, insights from $^{40}Ar/^{39}Ar$ ages on micas along a transect from Corsica to Tuscany. Tectonophysics 321:127–155

Capponi G, Crispini L (2002) Structural and metamorphic signature of alpine tectonics in the Voltri Massif (Ligurian Alps, northwestern Italy). Eclogae Geol Helv 95:31–42

Charrier G, Fernandez D, Malaroda R (1964) La formazione di Pianfolco (Bacino Oligocenico Ligure-Piemontese). Atti Acc Naz Lincei Ser 8, 7 Sez 2:25–81

Chiesa S, Cortesogno L, Forcella F, Galli M, Messiga B, Pasquarè G, Pedemonte GM, Piccardo GB, Rossi PM (1975) Assetto strutturale ed interpretazione geodinamica del Gruppo di Voltri. Boll Soc Geol Ital 94:555–582

Cimmino F, Messiga B, Piccardo GB (1979) Ti-clinohumite-bearing assemblages within antigoritic serpentinites of the Voltri Massif (Western Liguria): inferences on the geodynamic evolution of the piemontese ultramafic sections. Ofioliti 4:97–120

Cimmino F, Messiga B, Piccardo GB (1981) Le caratteristiche paragenetiche dell'evento di alta-pressione nei di.erenti sistemi (pelitici, femici, ultrafemici) delle ofioliti metamorfiche del Gruppo di Voltri (Liguria Occidentale). Rend Soc Ital Mineral Petrol 37:419–446

Compston W, Williams IS, Kirschvink JL, Zhang Z, Ma G (1992) Zircon U-Pb ages for the Early Cambrian time-scale. J Geol Soc Lond 149:171–184

Cortesogno L, Haccard D (1984) Note illustrative alla Carta geologica della Zona Sestri-Voltaggio. Mem Soc Geol Ital 18:115–150

Davidson A, van Breemen O (1988) Baddeleyite-zircon relationships in coronitic metagabbro, Grenville Province, Ontario: implications for geochronology. Contrib Mineral Petrol 100:291–299

Di Biase D, Pandolfi L (1999) L'evoluzione composizionale dei conglomerati della Val Borbera (Bacino Terziario Piemontese). Evidenze e vincoli per l'esumazione di unità a metamorfismo HP-LT nelle Alpi Occidentali. FIST Congress, Bellaria, Italy, Abstract Volume, pp 286–288

Di Biase D, Pandolfi L, Catanzariti R (2002) The sedimentary record of the mesoalpine orogenic wedge exhumation in the Lower Oligocene deposits of the Borbera Valley (eastern sector of the Tertiary Piedmont Basin). 81st Summer Meeting of the Italian Geological Society, Torino, Abstract Volume, pp 133–134

Dûchene S, Blichert-Toft J, Luais B, Télouk P, Lardeaux J-M, Albarède F (1997) The Lu-Hf dating of garnets and the ages of the Alpine high-pressure metamorphism. Nature 387:586–589

Eggins SM, Rudnick RL, McDonough WF (1998) The composition of peridotites and their minerals: a laser ablation ICP-MS study. Earth Planet Sci Lett 154:53–71

Ernst WG (1976) Mineral chemistry of eclogites and related rocks from the Voltri Group, Western Liguria, Italy. Schweiz Mineral Petrogr Mitt 56:292–343

Gebauer D, Schertl H-P, Brix M, Schreyer W (1997) 35-Ma-old ultrahigh-pressure metamorphism and evidence for very rapid exhumation in the Dora Maira Massif, Western Alps. Lithos 41:5–24

Gelati R, Gnaccolini M, Falletti P, Catrullo D (1993) Stratigrafia sequenziale della successione Oligo-Miocenica delle Langhe, bacino Terziario Ligure-Piemontese. Riv Ital Paleontol Stratigr 98:425–452

Gelati R, Gnaccolini M, Petrizzo MR (1998) Sedimentary tectonics and sedimentation in the Tertiary Piedmont Basin, northwestern Italy. Riv Ital Paleontol Stratigr 104:193–214

Harland WB, Armstrong RL, Cox AV, Craig LE, Smith AG, Smith DG (1989) A geological time scale. Cambridge University Press, Cambridge, 190 pp

Heaman LM, LeCheminant AN (1993) Paragenesis and U-Pb systematics of baddeleyite (ZrO2). Chem Geol 110:95–126

Hermann J, Muentener O, Scambelluri M (2000) The importance of serpentinite mylonites for subduction and exhumation of oceanic crust. Tectonophysics 327:225–238

Hinton RW, Upton BGJ (1991) The chemistry of zircon: variations within and between large crystals from syenite and alkali basalt xenoliths. Geochim Cosmochim Acta 55:3287–3302

Hoskin PWO, Black LP (2000) Metamorphic zircon formation by solid-state recrystallization of protolith igneous zircon. J Metamorph Geol 18:423–439

Inger S, Ramsbotham W, Cliff RA, Rex DC (1996) Metamorphic evolution of the Sesia-Lanzo Zone, Western Alps: time constraints from multi-system geochronology. Contrib Mineral Petrol 126:152–168

Liati A, Gebauer D (1999) Constraining the prograde and retrograde P–T-t path of Eocene HP rocks by SHRIMP dating different zircon domains: inferred rates of heating, burial, cooling and exhumation for central Rhodope, northern Greece. Contrib Mineral Petrol 135:340–354

Liati A, Gebauer D, Fanning M (2003) The youngest basic oceanic magmatism in the Alps (Late Cretaceous; Chiavenna uni, Central Alsp): geochronological constraints and geodynamic significance. Contrib Mineral Petrol 10.1007/s00410-003-0485-7

Liou JG, Zhang R, Ernst WG, Liu J, McLimans R (1998) Mineral parageneses in the Piampaludo eclogitic body, Gruppo di Voltri, Western Ligurian Alps. Schweiz Mineral Petrogr Mitt 78:317–335

Lombardo B, Rubatto D, Castelli D (2002) Ion microprobe U-Pb dating of zircon from a Monviso metaplagiogranite: implications for the evolution of the Piedmont-Ligurian Tethys in the Western Alps. Ofioliti 27:109–118

Lorenz C (1979) L'Oligo-Miocene Ligure: un example de trasgression. Bull Soc Géol Fr 4:375–378

Ludwig KR (2000) Isoplot/Ex version 2.4. A geochronological toolkit for Microsoft Excel. Berkeley, Berkeley Geochronological Centre Spec Publ, 56 pp

Messiga B (1987) Alpine metamorphic evolution of Ligurian Alps, north-western Italy: chemography and petrological constraints inferred from metamorphic climax assemblages. Contrib Mineral Petrol 85:269–277

Messiga B, Scambelluri M (1991) Retrograde P–T-t path from the Voltri Massif eclogites (Ligurian Alps, Italy): some tectonic implications. J Metamorph Geol 9:93–109

Messiga B, Tribuzio R, Bottazzi P, Ottolini L (1995) An ion microprobe study on trace element compositions of clinopyroxene from blueschist and eclogitized Fe-Ti gabbros, Ligurian Alps, northwestern Italy: some petrological considerations. Geochim Cosmochim Acta 59:59–75

Mottana A, Bocchio R (1975) Superferric eclogites of the Voltri Group (Penninic Belt, Apennines). Contrib Mineral Petrol 49:201–210

Paces JB, Miller JD (1993) U-Pb ages of the Duluth complex and related mafic intrusions, northeastern Minnesota: geochronologic insights into physical petrogenetic, paleomagnetic and

tectonomagmatic processes associated with the 1.1 Ga mid-continent rift system. J Geophys Res 98:13997–14013
Pidgeon RT (1992) Recrystallisation of oscillatory zoned zircon: some geochronological and petrological implications. Contrib Mineral Petrol 110:463–472
Pidgeon RT, Nemchin AA, Hitchen GJ (1998) Internal structures of zircons from Archean granites from the Darling Range batholith: implications for zircon stability and the interpretation of zircon U-Pb ages. Contrib Mineral Petrol 132:288–299
Polino R, Dal Piaz GV, Gosso G (1990) Tectonic erosion at the Adria margin and accretionary processes for the Cretaceous orogeny in the Alps. Mém Soc Géol Fr 156:345–367
Purtscheller F, Tessadri R (1985) Zirconolite and baddeleyite from metacarbonates of the Ötztal-Stubai complex (northern Tyrol, Austria). Mineral Mag 49:523–529
Rampone E, Hofmann AW, Piccardo GB, Vannucci R, Bottazzi P, Ottolini L (1995) Petrology, mineral and isotope geochemistry of the External Liguride peridotites (northern Apennines, Italy). J Petrol 36:81–105
Rampone E, Hofmann AW, Raczek I (1998) Isotopic contrasts within the Internal Liguride ophiolite (N. Italy): the lack of a genetic mantle-crust link. Earth Planet Sci Lett 163:175–189
Reischmann T, Brügmann GE, Jochum KP, Todt WA (1995) Trace element and isotopic composition of baddeleyite. Mineral Petrol 53:155–164
Rubatto D (2002) Zircon trace element geochemistry: distribution coefficients and the link between U-Pb ages and metamorphism. Chem Geol 184:123–138
Rubatto D, Gebauer D (1999) Eo/Oligocene (35 Ma) high-pressure metamorphism in the Monte Rosa nappe (western Alps): implications for paleogeography. Schweiz Mineral Petrogr Mitt 79:353–362
Rubatto D, Gebauer D, Compagnoni R (1999) Dating of eclogite-facies zircons: the age of Alpine metamorphism in the Sesia-Lanzo Zone (Western Alps). Earth Planet Sci Lett 167:141–158
Rubatto D, Gebauer D, Fanning M (1998) Jurassic formation and Eocene subduction of the Zermatt – Saas-Fee ophiolites: Implications for the geodynamic evolution of the Central and Western Alps. Contrib Mineral Petrol 132:269–287
Rubatto D, Hermann J (2001) Exhumation as fast as subduction? Geology 29:3–6
Rubatto D, Hermann J (2003) Zircon formation during fluid circulation in eclogites (Monviso, Western Alps): implications for Zr and Hf budget in subduction zones. Geochim Cosmochim Acta 67:2173–2187
Scambelluri M, Muentener O, Hermann J, Piccardo GB, Trommsdorff V (1995) Subduction of water into the mantle: history of an Alpine peridotite. Geology 23:459–462
Scambelluri M, Rampone E (1999) Mg-metasomatism of oceanic gabbros and its control on Ti-clinohumite formation during eclogitization. Contrib Mineral Petrol 135:1–17
Spalla MI, Lardeaux JM, Dal Piaz GV, Gosso G, Messiga B (1996) Tectonic significance of Alpine eclogites. J Geodyn 21:257–285
Stucki A, Trommsdorff V, Günther D (2001) Zirconolite in metarodingites of Penninic Mesozoic ophiolites, Central Alps. Schweiz Mineral Petrogr Mitt 81:257–265
Vavra G, Gebauer D, Schmidt R, Compston W (1996) Multiple zircon growth and recrystallization during polyphase Late Carboniferous to Triassic metamorphism in granulites of the Ivrea Zone (Southern Alps): an ion microprobe (SHRIMP) study. Contrib Mineral Petrol 122:337–358
Vavra G, Schmidt R, Gebauer D (1999) Internal morphology, habit and U-Th-Pb microanalysis of amphibolite-to-granulite facies zircons: geochronology of the Ivrea Zone (Southern Alps). Contrib Mineral Petrol 134:380–404
Vissers RLM, Drury MR, Hoogerduijn Strating EH, Van der Wal D (1991) Shear zones in the upper mantle: a case study in an Alpine lherzolite massif. Geology 19:990–993
Wingate MTD, Compston W (2000) Crystal orientation effects during ion microprobe U-Pb analysis of baddeleyite. Chem Geol 168:75–97